Space-Time Coded Systems using Continuous Phase Modulation

Rachel L. Maw, *Student Member, IEEE*, and Desmond P. Taylor, *Life Fellow, IEEE*

***Abstract*—We develop space-time trellis coded (STC) schemes using continuous-phase modulation (CPM). We employ the Rimoldi model of CPM to create a decomposed model of STC-CPM. The decomposition separates the coding from the modulation. The space-time encoding and the inherent CPM encoding is combined into a single trellis encoder on the ring of integers modulo-p. This is followed by a bank of memoryless modulators. The model allows the search for good space-time codes to take into account the inherent encoding of the modulation.**

***Index Terms*—Continuous phase modulation, space-time coding, ring convolutional codes.**

I. Introduction

SPACE-TIME coding (STC) has been widely used to reduce the effects of multipath fading [1], [2]. Most STC systems are based on linear modulations; however, it was shown in [3]–[6] that continuous phase modulation [7] (CPM) is a good alternative. Its constant envelope allows the use of low-cost power-efficient nonlinear amplifiers. The phase continuity implies that the modulation has memory or inherent coding and, therefore, a trellis representation.

Space-time code design with CPM has been investigated in [8] and [9], where design rules and code constructions for specific forms of CPM are derived that guarantee full spatial diversity. Trellis code design rules are presented in [10] for general constant envelope space-time modulation. Interleaved externally encoded STC-CPM systems have been developed in [11]–[13]. A reduced complexity receiver for layered space-time schemes with minimum-shift keying (MSK)-like modulations is presented in [14].

In this paper, an STC-CPM system that exploits the Rimoldi model [15] of CPM is developed for M-ary modulation with $M = p^{k_m}$, where p and k_m are positive integers. We assume a rational modulation index $h = q/p$, and form a decomposed model of STC-CPM. The resulting system consists of a convolutional encoder on the integer ring $\mathbb{Z}_p$ [16], [17], followed by a bank of L_t memoryless modulators, where L_t is the number of transmit antennas. This can be seen as an extension of the work in [18] and [19] to multiple transmit antenna schemes. Decoding is accomplished using the Viterbi algorithm on the trellis of the encoder. The STC-CPM encoder could be used as the inner code of an interleaved iteratively decoded structure [11]–[13]. In [20], serially concatenated CPM structures that utilize ring convolutional codes as the outer codes and CPM as the inner code are investigated for single thread systems.

The decomposition allows us to investigate code design for STC-CPM on an overall encoder trellis, which incorporates both the coding inherent to the modulation and that of the STC. For linearly modulated space-time trellis coded schemes, the code design criteria depend on ρL_r [21], [22], where L_r is the number of receive antennas and ρ is the minimum rank of the code word distance matrices with $\rho \leq L_t$. If $\rho L_r \leq 3$, the rank and the minimum determinant [1] of the distance matrices are the appropriate criteria. If $\rho L_r > 3$, the minimum trace of the code word distance matrices or, equivalently, the minimum squared Euclidean distance ($d^2_{\min}$) between the transmitted signals is better used [21], [22]. Directly analogous results apply to STC-CPM, if the signal distance matrix [9] is considered.[1] The rank, determinant and $d^2_{\min}$ criteria then hold for STC-CPM. Using the decomposed model, we may derive an expression for $d^2_{\min}$ based on the trellis of the overall encoder [5].

We give a brief overview of CPM in the following section. We then develop the STC-CPM system model. Simulated performance curves are presented and discussed in Section IV.

II. Continuous Phase Modulation

A CPM signal [7], [15] can be described by

$$s(t, \boldsymbol{X}(D)) = \sqrt{\frac{2E}{T}} \cos(2\pi f_1 t + \tilde{\psi}(t, \boldsymbol{X}(D)) + \psi_o) \qquad nT \leq t \leq (n+1)T \quad (1)$$

where $f_1 = f_c - (M-1)h/2T$ is the asymmetric carrier frequency, f_c is the carrier frequency, E is the symbol energy, T is the symbol period, ψ_o is the initial phase offset,[2] and the M-ary data sequence $\boldsymbol{U}$ has elements $U_n \in \{0, 1, \ldots, (M-1)\}$. The information carrying or physical tilted phase is given by

$$\tilde{\psi}(t, \boldsymbol{X}(D)) = \left(2\pi h \left[\sum_{i=0}^{n-L} U_i \right] \bmod p + 4\pi h \sum_{i=n}^{n-L+1} U_i q(t - iT) + W(t) \right) \bmod (2\pi), \qquad nT \leq t \leq (n+1)T \quad (2)$$

[1] We note that in any practical sense, CPM signals and codes are indistinguishable since the phase variation within each interval defines the code and, hence, the distance matrix.

[2] This is set arbitrarily to zero in what follows.

Paper approved by H. Jafarkhani, the Editor for Modulation/Detection of the IEEE Communications Society. Manuscript received July 17, 2006; revised November 21, 2006. This work was supported in part by the Bright Futures Scholarship Scheme administered by the New Zealand Tertiary Education Commission and in part by the Foundation for Research, Science and Technology. This paper was presented in part at the WIRELESSCOM, Maui, HI, June 2005 and at GLOBECOM, St. Louis, MO, November 2005.

The authors are with the Department of Electrical and Computer Engineering, University of Canterbury, Christchurch 8140, New Zealand (e-mail: rlm57@student.canterbury.ac.nz; taylor@elec.canterbury.ac.nz).

Digital Object Identifier 10.1109/TCOMM.2007.908508

where $h = q/p$ is the modulation index, $W(t)$ is the sum of data independent terms, and $q(t)$ is the phase function. Function $q(t)$ is the integral of the instantaneous frequency response and has a duration of LT [15]. From (2), we see that the output of the modulator is specified by the vector

$$\boldsymbol{X}_n = [U_n, \ldots, U_{n-L+1}, V_n], \quad nT \le t \le (n+1)T \tag{4}$$

where

$$V_n = \left[\sum_{i=0}^{n-L} U_i\right] \bmod p = [V_{n-1} + U_{n-L}] \bmod p, \quad nT \le t \le (n+1)T. \tag{5}$$

CPM can thus be represented by a pM^{L-1} state time-invariant phase trellis.

We may represent the M-ary ($M = p^{k_m}$) input symbols in radix-p form as

$$U_n = \sum_{j=1}^{k_m} U_n^j p^{k_m - j}, \qquad nT \le t \le (n+1)T \tag{6}$$

where the subsymbols U_n^j are on $\mathbb{Z}_p$. We denote the jth subsymbol sequence as $\boldsymbol{U}^j(D) = U_0^j + U_1^j D + \cdots + U_n^j D^n + \cdots$, where D represents a unit delay. A convolutional encoder on $\mathbb{Z}_p$ can then generate $\boldsymbol{X}(D) = \boldsymbol{X}_0 + \boldsymbol{X}_1 D + \cdots + \boldsymbol{X}_n D^n + \cdots$, to form the input to a time-invariant memoryless modulator that outputs $s(t, \boldsymbol{X}(D))$. This encoder encodes the sequences $\boldsymbol{U}(D) = [\boldsymbol{U}^1(D) \quad \boldsymbol{U}^2(D) \ldots \boldsymbol{U}^{k_m}(D)]$, and has the $k_m \times (k_m L + 1)$ generator matrix given by (3), where $\boldsymbol{0}_{i,j}$ represents an $(i \times j)$ matrix of zeroes. The output of the encoder is related to the input by $\boldsymbol{X}(D) = \boldsymbol{C}(D)\boldsymbol{U}(D)$.

To avoid catastrophic codes in what follows, we use a precoder as in [18] and [23] to cancel the feedback term in $\boldsymbol{C}(D)$. The precoder generator matrix is given by

$$\boldsymbol{T}(D) = \begin{bmatrix} \boldsymbol{I}_{k_m - 1} & \boldsymbol{0}_{k_m - 1,1} \\ \boldsymbol{0}_{1,k_m - 1} & 1 - D \end{bmatrix} \tag{7}$$

where $\boldsymbol{I}_i$ is the $(i \times i)$ identity matrix. $\boldsymbol{T}(D)$ is cascaded with $\boldsymbol{C}(D)$ to create a feedback-free CPE (FF-CPE) with the generator matrix $\boldsymbol{W}(D) = \boldsymbol{T}(D)\boldsymbol{C}(D)$.

III. STC-CPM

The proposed space-time coded CPM transmitter structure is shown in Fig. 1. We let L_t and L_r denote the number of transmit antennas and receive antennas, respectively. We define the space-time encoder as a linear rate-k/l convolutional encoder on the integer ring $\mathbb{Z}_p$, where k, l are integers and $l \ge k$. The

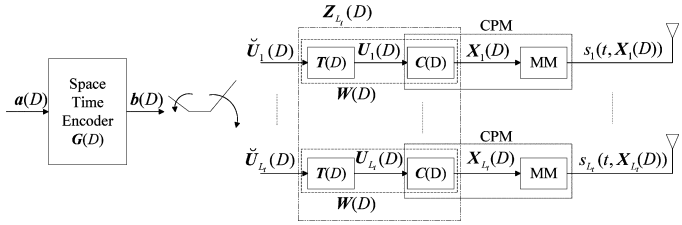

Fig. 1. Block diagram of the STC-CPM transmitter.

space-time encoder is followed by a commutator that produces the input sequences for the L_t FF-CPEs. The p-ary data sequence $\boldsymbol{a}(D) = \boldsymbol{a}_0 + \boldsymbol{a}_1 D + \cdots + \boldsymbol{a}_j D^j + \cdots$ is input into the space-time encoder, which has generator matrix $\boldsymbol{G}(D)$. During the interval $jT_{k_v} \le t \le (j+1)T_{k_v}$, the input is $\boldsymbol{a}_j = [a_j^1 \;\; a_j^2 \cdots a_j^k]$. The space-time encoder output is then

$$\boldsymbol{b}(D) = \boldsymbol{a}(D)\boldsymbol{G}(D) \tag{8}$$

where $\boldsymbol{b}(D) = \boldsymbol{b}_0 + \boldsymbol{b}_1 D + \cdots + \boldsymbol{b}_j D^j + \cdots$ and $\boldsymbol{b}_j = [b_j^1 b_j^2 \cdots b_j^l]$ is output during the interval $jT_{k_v} \le t \le (j+1)T_{k_v}$.

The commutator groups the STC output symbols into L_t blocks, each containing k_m p-ary symbols to form the input for the FF-CPEs. During the nth symbol interval of duration $T = (T_{k_v} k_m L_t)/l$, the resulting $k_m L_t$ dimensional vector of p-ary symbols is given by

$$\breve{\boldsymbol{U}}_n = [\breve{\boldsymbol{U}}_{1,n} \; \breve{\boldsymbol{U}}_{2,n} \; \cdots \; \breve{\boldsymbol{U}}_{L_t,n}], \quad nT \le t \le (n+1)T \tag{9}$$

where each subvector

$$\breve{\boldsymbol{U}}_{i,n} = \left[\breve{U}_{i,n}^1 \; \breve{U}_{i,n}^2 \; \cdots \; \breve{U}_{i,n}^{k_m}\right], \qquad i = 1, 2, \ldots, L_t \tag{10}$$

consists of the k_m coefficients of the radix-p expression of (6). A subvector forms one M-ary channel symbol. The output sequence of the ith FF-CPE may then be written as

$$\boldsymbol{U}_i(D) = \breve{\boldsymbol{U}}_i(D)\boldsymbol{W}(D), \qquad i = 1, 2, \ldots, L_t \tag{11}$$

where $\breve{\boldsymbol{U}}_i(D) = \breve{\boldsymbol{U}}_{i,0} + \breve{\boldsymbol{U}}_{i,1} D + \cdots + \breve{\boldsymbol{U}}_{i,j} D^j + \cdots$ and $\boldsymbol{X}_i(D) = \boldsymbol{X}_{i,0} + \boldsymbol{X}_{i,1} D + \cdots + \boldsymbol{X}_{i,j} D^j + \cdots$, so that the $Lk_m + 1$-symbol vector output during the nth symbol interval is given by

$$\boldsymbol{X}_{i,n} = \left[X_{i,n}^{1,1} \; \cdots \; X_{i,n}^{1,k_m} \; X_{i,n}^{2,1} \; \cdots \; X_{i,n}^{L,k_m} \; X_{i,n}^{L+1,1}\right] \quad nT \le t \le (n+1)T. \tag{12}$$

The signal $s_i(t, \boldsymbol{X}_i(D))$ is transmitted from the antenna i. The throughput of the overall system is $(k \log_2(p) k_m L_t)/l$ bits per channel use.

$$\boldsymbol{C}(D) = \begin{bmatrix} 1 & D & D^2 & \ldots & D^{L-1} & \boldsymbol{0}_{1,L} & & \cdots & & \boldsymbol{0}_{1,L+1} \\ & & \boldsymbol{0}_{1,L} & & \ddots & & \boldsymbol{0}_{1,L} & & \vdots & \\ & & \boldsymbol{0}_{1,L} & & \boldsymbol{0}_{1,L} & 1 & D & D^2 \; \ldots \; D^{L-1} & \boldsymbol{0}_{1,L+1} & \\ & & \boldsymbol{0}_{1,L} & & \cdots & & \boldsymbol{0}_{1,L} & & 1 \quad D \quad D^2 \; \ldots \; D^{L-1} & \dfrac{D^L}{1-D} \end{bmatrix} \tag{3}$$

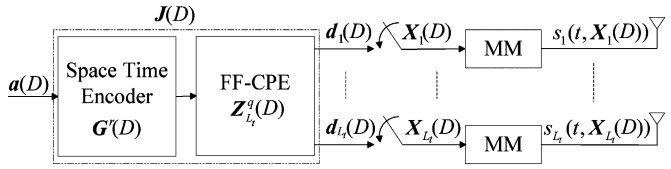

Fig. 2. Block diagram of the combined STC-CPM encoder.

We can combine the L_t feedback-free CPEs $\boldsymbol{W}(D)$ into a single encoder with the $k_m L_t \times (k_m L + 1)L_t$ generator matrix $\boldsymbol{Z}_{L_t}(D)$

$$= \begin{bmatrix} \boldsymbol{W}(D) & \mathbf{0}_{k_m,k_m L+1} & \cdots & \mathbf{0}_{k_m,k_m L+1} \\ \mathbf{0}_{k_m,k_m L+1} & \ddots & \ddots & \vdots \\ \vdots & \ddots & \boldsymbol{W}(D) & \mathbf{0}_{k_m,k_m L+1} \\ \mathbf{0}_{k_m,k_m L+1} & \cdots & \mathbf{0}_{k_m,k_m L+1} & \boldsymbol{W}(D) \end{bmatrix}. \tag{13}$$

During the nth symbol interval, the input to $\boldsymbol{Z}_{L_t}(D)$ is the $k_m L_t$ dimensional vector $\breve{\boldsymbol{U}}_n$ and the output is the $(k_m L + 1)L_t$ dimensional vector

$$\boldsymbol{X}_n = \left[\boldsymbol{X}_{1,n}\ \boldsymbol{X}_{2,n}\ \cdots\ \boldsymbol{X}_{L_t,n}\right], \qquad nT \le t \le (n+1)T. \tag{14}$$

We may combine $\boldsymbol{Z}_{L_t}(D)$ with the space-time encoder $\boldsymbol{G}(D)$ to obtain an encoder that incorporates the entire encoding process. If the rate-k/l space-time encoder is designed such that $l = k_m L_t$, $\boldsymbol{G}(D)$ can be directly cascaded with $\boldsymbol{Z}_{L_t}(D)$. The overall generator matrix is then

$$\boldsymbol{J}(D) = \boldsymbol{G}(D)\boldsymbol{Z}_{L_t}(D). \tag{15}$$

If $l \neq k_m L_t$, we must effectively move the commutator to follow the encoding as shown in Fig. 2. To do this, we find the lowest common multiple of l and $k_m L_t$, such that $rl = qk_m L_t$, where r and q are integers. We convert $\boldsymbol{G}(D)$ to the rate-rk/rl matrix $\boldsymbol{G}^r(D)$ and $\boldsymbol{Z}_{L_t}(D)$ to the rate-$qk_m L_t/qL_t(k_m L + 1)$ matrix $\boldsymbol{Z}^q_{L_t}(D)$. These may be directly cascaded to obtain the composite encoder $\boldsymbol{J}(D) = \boldsymbol{G}^r(D)\boldsymbol{Z}^q_{L_t}(D)$ that has an $rk \times qL_t(k_m L + 1)$ generator matrix. Only one rate conversion is required if l is a multiple of $k_m L_t$ or vice versa. The encoder $\boldsymbol{G}^r(D)$ accepts the rk-symbol input vector

$$\boldsymbol{a}_j = \left[\mathrm{a}_j^1\ a_j^2\ \cdots\ a_j^{rk}\right], \qquad jT_{k_f} \le t \le (j+1)T_{k_f} \tag{16}$$

and outputs an rl-symbol vector denoted $\boldsymbol{c}_j$ every T_{k_f}-second interval, where $T_{k_f} = rT_{k_v} = Tq$. Similarly, the encoder $\boldsymbol{Z}^q_{L_t}(D)$ accepts the $qk_m L_t = rl$-symbol vector $\boldsymbol{c}_j$, output from $\boldsymbol{G}^r(D)$, and produces a $qL_t(k_m L + 1)$-symbol vector given by

$$\boldsymbol{d}_j = [\boldsymbol{d}_{1,j}\ \boldsymbol{d}_{2,j}\ \cdots\ \boldsymbol{d}_{L_t,j}], \qquad jT_{k_f} \le t \le (j+1)T_{k_f} \tag{17}$$

every T_{k_f}-second interval, where

$$\begin{aligned} \boldsymbol{d}_{i,j} &= \left[d_{i,j}^1\ d_{i,j}^2\ \cdots\ d_{i,j}^{q(k_m L+1)}\right] \\ &= \left[\boldsymbol{X}_{i,jq}\ \boldsymbol{X}_{i,jq+1}\ \cdots\ \boldsymbol{X}_{i,(j+1)q-1}\right], \\ &\qquad i = 1,2,\ldots,L_t, \quad jT_{k_f} \le t \le (j+1)T_{k_f} \end{aligned} \tag{18}$$

and

$$\begin{aligned} \boldsymbol{X}_{i,n} = \big[&d_{i,j}^{(n-jq)(k_m L+1)+1}\ d_{i,j}^{(n-jq)(k_m L+1)+2} \\ &\cdots\ d_{i,j}^{(n-jq+1)(k_m L+1)}\big], \qquad jq \le n \le (j+1)q-1, \\ &jT_{k_f} \le t \le (j+1)T_{k_f}. \end{aligned} \tag{19}$$

We can easily find $\boldsymbol{G}^r(D)$ and $\boldsymbol{Z}^q_{L_t}(D)$ using the method in [18]. The overall encoder input during the interval $jT_{k_f} \le t \le (j+1)T_{k_f}$ is $\boldsymbol{a}_j$ and its output is $\boldsymbol{d}_j$. During the nth symbol interval ($T = \frac{T_{k_f}}{q}$), the ith sampler selects the $Lk_m + 1$-symbol vector $\boldsymbol{X}_{i,n}$, which is input into the ith memoryless modulator.

A. Overall Encoder Complexity

The number of states in the overall trellis is given by

$$S_J = S_G n_s \le S_G S_Z \tag{20}$$

where S_G and $S_Z = (pM^{L-1})^{L_t}$ are the number of states of the encoders $\boldsymbol{G}^r(D)$ and $\boldsymbol{Z}^q_{L_t}(D)$, respectively. The value of n_s is determined by how the states of the encoders $\boldsymbol{G}^r(D)$ and $\boldsymbol{Z}^q_{L_t}(D)$ merge in the overall trellis [18], [23].

We now consider the number of states in the overall encoder for the special case of full response ($L = 1$) CPM, where $n_s \le p^{L_t}$. We assume that the space-time encoder is rate-k/l and that l is a multiple of $k_m L_t$, such that $l = qk_m L_t$. Then, n_s is equal to the number of possible combinations that the L_t elements $\{c_j^{qk_m}, c_j^{2qk_m}, \ldots, c_j^{L_t qk_m}\}$ of the space-time encoder output vector ($\boldsymbol{c}_j$) can take on before the space-time encoder merges to the zero state.

IV. Simulation Results and Discussion

The simulations were run using a frame length of 130 symbols. Each receive antenna receives a faded superposition of the L_t simultaneously transmitted signals corrupted by additive white Gaussian noise (AWGN). The fading is assumed to be slow Rayleigh flat fading, such that the $L_t L_r$ fading gains are constant during a frame, but vary from frame to frame. The random fading gain between each transmit and receive antenna during a frame is modeled as an independent complex Gaussian random variable with zero mean and a variance of 1/2 per dimension. The AWGN noise component is an independent sample of a zero-mean complex Gaussian random process, with power spectral density N_0. The receiver implements matched filtering and decodes on the overall trellis using the Viterbi algorithm. Perfect channel state information is assumed at the receiver. For simplicity, we restrict the simulations to continuous phase frequency shift keying (CPFSK), a full response CPM ($L = 1$) with a rectangular frequency pulse.

Fig. 3 shows the frame error rate performance of 4-ary CPFSK schemes with two transmit antennas. The space-time codes are $\boldsymbol{G}(D) = [1\ \frac{1}{1+2D}]$, $\boldsymbol{G}(D) = [D\ 1]$, and $\boldsymbol{G}(D) = [1\ \frac{1+2D}{1+D}]$. The rank ($\rho$) of the signal distance matrix for $\boldsymbol{G}(D) = [1\ \frac{1}{1+2D}]$ is unity and $d^2_{\min} = 2.88$. Here, $S_G = 4$ and $n_s = 2$, and hence, the STC-CPFSK scheme has an 8-state trellis. The code $\boldsymbol{G}(D) = [D\ 1]$, which is also known as

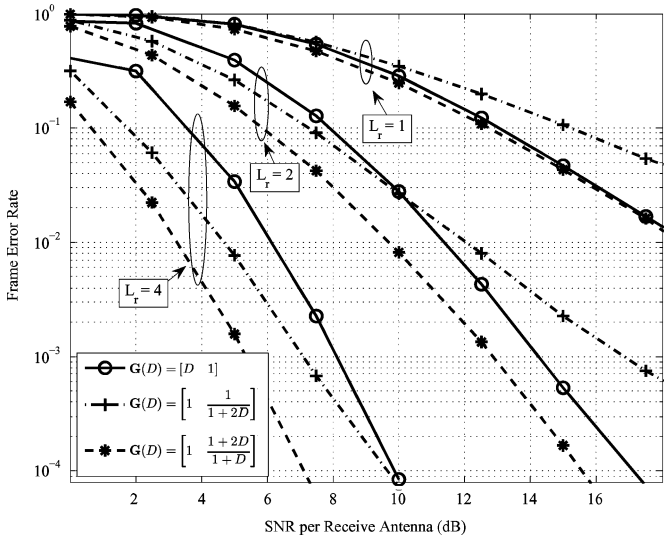

Fig. 3. Frame error rate performance of two transmit antenna systems with 4-CPFSK and one, two, and four receive antennas. The space-time codes are $\boldsymbol{G}(D) = [D\ 1]$ ($\circ$), $\boldsymbol{G}(D) = [1\ \frac{1}{1+2D}]$ ($+$), and $\boldsymbol{G}(D) = [1\ \frac{1+2D}{1+D}]$ ($*$).

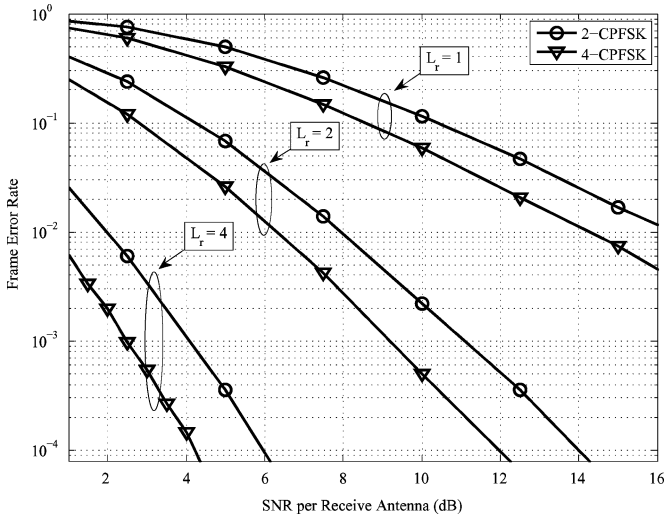

Fig. 4. Frame error rate performance of rate-1 two transmit antenna systems. The systems are 2-CPFSK with $\boldsymbol{G}(D) = [D\ 1]$ ($\circ$) and 4-CPFSK with $\boldsymbol{G}(D) = [2 + 3D + 2D^2\ \ 1 + D\ \ 2 + 2D^2\ \ \frac{3+2D^2}{1+D}]$ (∇) with one, two, and four receive antennas. Both systems yield the same throughput.

delay diversity, is a full rank code ($\rho = 2$) with $d^2_{\min} = 1.45$ and a 16-state overall trellis ($S_G = 4, n_s = 4$). The code $\boldsymbol{G}(D) = [1\ \frac{1+2D}{1+D}]$ is also full rank and has a 16-state trellis ($S_G = 4, n_s = 4$) with $d^2_{\min} = 3.24$. The results are presented for one, two, and four receive antennas.

When $\rho L_r \geq 4, d^2_{\min}$ dominates the error performance. For $\boldsymbol{G}(D) = [1\ \frac{1}{1+2D}]$, this holds if $L_r \geq 4$ and for both the rank-2 codes if $L_r \geq 2$. The slopes of the frame error curves of the rank-1 STC are less steep than those of the rank-2 codes. However, for $L_r = 4$, the rank-1 code outperforms the full rank delay diversity system for FER $< 10^{-4}$. The two rank-2 codes have similar performance with one receive antenna. As expected, for $L_r \geq 2$ receive antennas, $\boldsymbol{G}(D) = [1\ \frac{1+2D}{1+D}]$ with a larger value of $d^2_{\min}$ has superior performance.

As a further example, we consider the rate-$\frac{1}{4}$ space-time code $\boldsymbol{G}(D) = [2 + 3D + 2D^2\ \ 1 + D\ \ 2 + 2D^2\ \ \frac{3+2D^2}{1+D}]$ with 4-ary CPFSK and $L_t = 2$. This system has a throughput of 1 bit per channel use. The space-time encoder has M^3 states, and with $L_t = 2$ and CPFSK, the variable $n_s = 1$. The overall encoder with 4-ary CPFSK then has 64 states. The Euclidean distance of the scheme is 6.94 compared to 2 for delay diversity with 2-ary CPFSK (which has the same rank and throughput) and its frame error rate performance is significantly better as shown in Fig. 4. The cost of the improvement is the number of states in the overall trellis, i.e., 64 compared to 4. The bit error rate performance (not shown) of the more complex code is worse than for delay diversity when $L_r = 1$ and better when $L_r \geq 2$, this is attributable to the system having $\rho L_r < 4$ for $L_r = 1$.

V. Conclusion

In this paper, we have developed an STC-CPM model that allows the space-time encoder and the continuous phase encoders to be simply combined into a single trellis encoder. This can easily be extended to incorporate external error correction encoding of the same form. The STC-CPM codes can be used as the inner code of an interleaved iteratively decoded system. The model makes it straightforward to calculate $d^2_{\min}$, which is important for code design when $\rho L_r \geq 4$. Simulation results of selected STC-CPFSK systems are presented. These illustrate the importance of $d^2_{\min}$ and the rank of the signal distance matrix.

References

[1] V. Tarokh, N. Seshadri, and A. R. Calderbank, "Space-time codes for high data rate wireless communication: Performance analysis and code construction," *IEEE Trans. Inf. Theory*, vol. 44, no. 2, pp. 744–765, Mar. 1998.

[2] J.-C. Guey, M. P. Fitz, M. R. Bell, and W.-Y. Kuo, "Signal design for transmitter diversity wireless communication systems over Rayleigh fading channels," in *Proc. Veh. Tech. Conf.*, vol. 46, Atlanta, GA, 1996, pp. 136–140.

[3] X. Zhang and M. P. Fitz, "Constant envelope space-time modems," in *Proc. Veh. Tech. Conf.*, Oct. 2003, vol. 3, pp. 1772–1776.

[4] J. K. Cavers, "Space-time coding using MSK," *IEEE Trans. Wireless Commun.*, vol. 4, no. 1, pp. 185–191, Jan. 2005.

[5] R. L. Maw and D. P. Taylor, "Externally encoded space-time coded systems with continuous phase frequency shift keying," in *Proc. Int. Conf. Wireless Netw., Commun. Mobile Comput.*, Jun. 2005, vol. 2, pp. 1597–1602.

[6] R. L. Maw and D. P. Taylor, "Space-time coded systems with continuous phase frequency shift keying," in *Proc. Global Telecommun. Conf.*, Nov. 2005, vol. 3, pp. 1581–1586.

[7] J. B. Anderson, T. Aulin, and C.-E. W. Sundberg, *Digital Phase Modulation*. New York: Plenum, 1986.

[8] X. Zhang and M. P. Fitz, "Space-time code design with CPM transmission," in *Proc. Int. Symp. Inf. Theory*, Washington, DC, Jun. 2001, p. 327.

[9] X. Zhang and M. P. Fitz, "Space-time code design with continuous phase modulation," *IEEE J. Sel. Areas Commun.*, vol. 21, no. 5, pp. 783–792, Jun. 2003.

[10] J. Sykora, "Constant envelope space-time modulation trellis code design for Rayleigh flat fading channel," in *Proc. Global Telecommun. Conf.*, San Antonio, TX, 2001, vol. 2, pp. 1113–1117.

[11] X. Zhang and M. P. Fitz, "Soft-output demodulator in space-time-coded continuous phase modulation," *IEEE Trans. Signal Process.*, vol. 50, no. 10, pp. 2589–2598, Oct. 2002.

[12] C.-C. Chen and C.-C. Lu, "Space-time code design for CPFSK modulation over frequency-nonslective fading channels," *IEEE Trans. Commun.*, vol. 53, no. 9, pp. 1477–1489, Sep. 2005.
[13] D. Bokolamulla and T. M. Aulin, "Performance of space-time coded continuous phase modulated signals over different fading environments," in *Proc. Int. Symp. Inf. Theory*, Sep. 2005, pp. 1048–1052.
[14] W. Zhao and G. B. Giannakis, "Reduced complexity receivers for layered space-time CPM," in *IEEE Trans. Wireless Commun.*, vol. 4, no. 2, pp. 574–582, Mar. 2005.
[15] B. E. Rimoldi, "A decomposition approach to CPM," *IEEE Trans. Inf. Theory*, vol. 34, no. 2, pp. 260–270, Mar. 1988.
[16] J. L. Massey and T. Mittelholzer, "Convolutional codes over rings," in *Proc. 4th Joint Swedish-USSR Workshop Inf. Theory*, Gotland, Sweden, Aug.–Sep. 1989, pp. 14–18.
[17] J. L. Massey and T. Mittelholzer, "Systematicity and rotational invariance of convolutional codes over rings," in *Proc. 2nd Int. Workshop Algebraic Combinatorial Coding Theory*, Leningrad, Russia, Sep.1990, pp. 154–159.
[18] R. H.-H. Yang and D. P. Taylor, "Trellis-coded continuous-phase frequency-shift keying with ring convolutional codes," *IEEE Trans. Inf. Theory*, vol. 40, no. 4, pp. 1057–1067, Jul. 1994.
[19] B. E. Rimoldi and Q. Li, "Coded continuous phase modulation using ring convolutional codes," *IEEE Trans. Commun.*, vol. 43, no. 11, pp. 2714–2720, Nov. 1995.
[20] M. Xiao and T. M. Aulin, "Serially concatenated continuous phase modulation with convolutional codes over rings," *IEEE Trans. Commun.*, vol. 54, no. 8, pp. 1387–1395, Aug. 2006.
[21] Z. Chen, J. Yuan, and B. Vucetic, "An improved space-time trellis coded modulation scheme on slow Rayleigh fading channels," in *Proc. Int. Conf. Commun.*, Jun. 2001, vol. 4, pp. 1110–1116.
[22] B. Vucetic and J. Yuan, *Space-Time Coding*. Chichester: Wiley, 2003.
[23] F. Morales-Moreno, W. Holubowicz, and S. Pasupathy, "Optimization of trellis coded TFM via matched codes," *IEEE Trans. Commun.*, vol. 42, no. 2–4, pp. 1586–1594, Feb./Mar./Apr. 1994.